

# Sloped-Wall Thin-Film Photonic Crystal Waveguides

Juan A. Monsoriu, Enrique Silvestre, Albert Ferrando, Pedro Andrés, and Miguel V. Andrés

**Abstract**—The effect of the slope of the groove walls in the behavior of thin-film one-dimensional photonic crystal waveguides is extensively studied. In this respect, we point out its influence on the modal dispersion relations and then on the bandgap structure in general. Likewise, we also prove the lack of accuracy in the evaluation of the bandgap edges when material dispersion is ignored. The extreme importance of both facts, the wall slope and the material dispersion, in the analysis and design of realistic photonic crystal devices is emphasized. In particular, we exploit the wall slope as a new design parameter. By suitably choosing the value of the above parameter, sloped-wall photonic crystal waveguides with high quality factor or high group velocity dispersion can be achieved.

**Index Terms**—Group velocity dispersion, integrated optics, optical waveguides, photonic crystals, vertical asymmetry.

THERE IS a great deal of interest in the properties of photonic crystals fabricated in the form of thin films, commonly called photonic crystal waveguides [1], [2]. Like bulk photonic crystals, these structures are designed to control the emission and propagation of light, mostly to increase the functionality of electrooptic and telecommunication devices, constituting microlasers [3] or dispersion compensators [4], [5].

Today, fabrication techniques are good enough to control, with high fidelity and repeatability the practical realization of such structures [6]. On the contrary, roughly speaking, design tools are not very accurate and reliable, materials are assumed to be nondispersive, and some systematic deviations between the geometry of the real device and that of the ideal one are not taking into account. Specifically, vertical walls tend to be tilted [7], holes are cylindroconical [8], and interfaces exhibit some degree of roughness [9].

In this letter, we describe the effect of sloped walls, together with material dispersion, in the behavior of thin-film one-dimensional (1-D) photonic crystal waveguides. The study carried out below allows us to infer that an accurate description of such structures is mandatory to reproduce the behavior of realistic devices. Perhaps the most obvious consequence is the deviation one obtains when the limits of the photonic bandgaps are evaluated. This shift has also been detected when other nonideal photonic crystal waveguides with hole-size nonuniformities [10] or

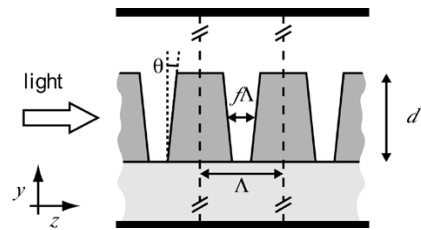


Fig. 1. Schematic diagram of the 1-D photonic crystal waveguide under consideration, in which guided light propagates along the  $z$  axis. The walls of the grooves etched in the high-index thin film are tilted an angle  $\theta$ . The two dashed lines together with the metallic plates (thick solid lines), inserted for computational purposes, bound the integration domain.

with a certain state of disorder on the position of the elementary microstructures [11] are considered.

Going one step further, recently the use of stepped walls in photonic-crystal-film defects has been proposed to control the emission of light [12]. In our case, we demonstrate that the wall tilt could be used as a new design parameter that modify the position and width of the bandgap. In the same direction, we also show the effect of the wall tilt on both the group velocity dispersion of the waveguide and the quality factor of the photonic thin film working as a vertical cavity.

First we analyze the waveguiding structure depicted in Fig. 1. It consists of a thin film of  $\text{Al}_x\text{Ga}_{1-x}\text{As}$ , with refractive index 3.45, and a substrate of oxidized  $\text{Al}_y\text{Ga}_{1-y}\text{As}$  with index 1.57, air being the cover. The film of thickness  $d$  is etched with a 1-D lattice of grooves with period  $\Lambda = 2d/3$  and air-filling fraction  $f$ . We have considered tilts of the groove walls between  $\theta = 0$  (vertical walls) and  $7.5^\circ$ .

The numerical technique employed to calculate the guided modes in this kind of structure is based on a modal algorithm that allows us to simulate three-dimensional (3-D) dielectric systems [13]. The key idea of the method consists in expanding the 3-D wave equation for the magnetic field in a certain domain in terms of the modes of an auxiliary system properly selected to provide a suitable basis.

In the present case, we consider the system periodic along the propagation direction ( $z$  axis), and therefore, we must select periodic boundary conditions in such a direction, whereas we permit the boundary to be confining in the direction perpendicular to the film plane ( $y$  axis). This implies that, for computational purposes, the photonic crystal waveguide is placed between two parallel perfectly conducting metallic plates (see Fig. 1). In this way, the auxiliary system we choose is the 1-D homogeneous air-filled metallic waveguide resulting from the removal of the photonic crystal slab, whose modes are well known. Since we are only interested in the analysis of guided modes, whose existence in photonic crystal waveguides has been verified experimentally [14], here it is not necessary to include, for instance, an absorbing layer against the conducting

Manuscript received June 10, 2004; revised October 8, 2004. This work was supported by the Ministerio de Ciencia y Tecnología, Spain (Grant TIC2002-04527-C02-02), and by the Generalitat Valenciana, Spain (Grant Grupos03/227).

J. A. Monsoriu is with the Departamento de Física Aplicada, Universidad Politécnica de Valencia, 46022 Valencia, Spain.

E. Silvestre, A. Ferrando, and P. Andrés are with the Departamento de Óptica, Universidad de Valencia, 46100 Burjassot (Valencia), Spain (e-mail: enrique.silvestre@uv.es).

M. V. Andrés is with the Departamento de Física Aplicada, Universidad de Valencia, 46100 Valencia, Spain, and also with the Institut de Ciència dels Materials, Universidad de Valencia, 46100 Burjassot (Valencia), Spain.

Digital Object Identifier 10.1109/LPT.2004.840828

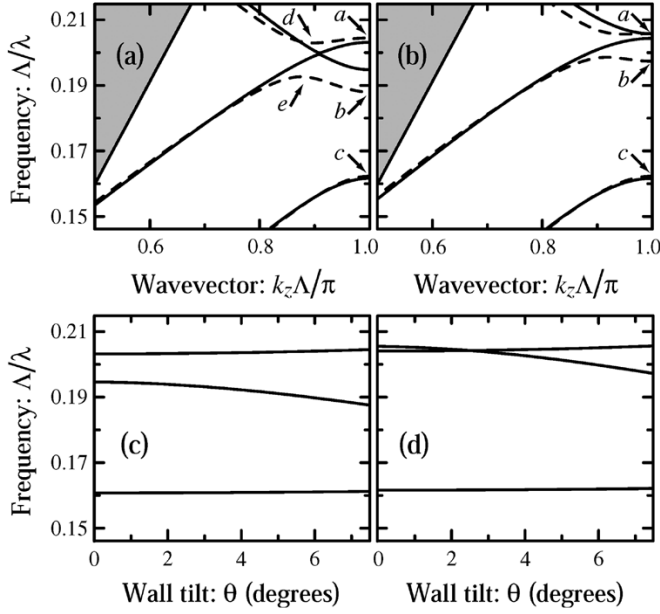


Fig. 2. TE Brillouin diagram for two air-filling fractions: (a)  $f = 0.20$  and (b)  $f = 0.25$ . In each one of these two figures, we plot the results for vertical walls (solid lines) and for sloped walls with  $\theta = 7.5^\circ$  (dashed lines). The shaded regions correspond to radiation modes. Additionally, the frequency of the guided modes versus wall tilt at the edge of the first Brillouin zone, i.e.,  $k_z = \pi/\Lambda$ , is also plotted for (c)  $f = 0.20$ , and (d)  $f = 0.25$ .

plates to deal with the continuous part of the spectrum. It suffices to place the bounding metallic plates far enough from the photonic crystal film. It is worthwhile to point out that the staircase approximation used in other approaches, such as scattering and coupled wave methods, could provide the wrong results, as it has been proved for arbitrary-shaped diffraction gratings [15].

Fig. 2(a) and (b) shows the transverse-electric (TE) Brillouin diagram for the structure sketched in Fig. 1 with two different air-filling fractions,  $f = 0.20$  and  $0.25$ , respectively, and two wall tilts. The case for  $f = 0.20$  and vertical wall grooves was previously published by Atkin *et al.* [2], who analyzed the mode-mixing at the anticrossing points (d) and (e). Inspection of Fig. 2(a) and (b) reveals that tilted walls, due to a stronger coupling between modes, generate important changes at the photonic bandgap limits. In particular, in those diagrams, we can observe a noticeable widening of the bandgap with  $\theta$ , instead of doing it with  $f$ , as it could be expected. In order to point out this fact, in Fig. 2(c) and (d), we show the variation of the mode frequency as a function of  $\theta$  at the edge of the first Brillouin zone. We conclude that it is crucial to carry out an accurate description of the device geometry when studying realistic systems. It is worthwhile to notice that in the nondispersive-material calculations carried out up to now, only the dimensionless quantities  $f$ ,  $\Lambda/\lambda$ ,  $\Lambda k_z$ , and  $\Lambda/d$  are relevant. Subsequently, the inclusion of material dispersion in the analysis breaks the scale invariance of the equations, losing, therefore, the universality that the bandgap diagrams had.

In addition to the remarkable widening of the bandgap, a significant reduction in the curvature of the dispersion curves at the band edge is also produced. This fact involves the increase in the quality factor  $Q$  of the film operating as a vertical micro-

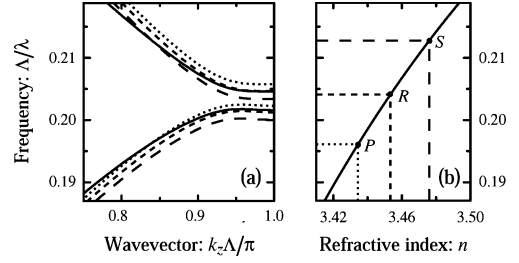


Fig. 3. (a) Detail of the TE Brillouin diagram for  $\theta = 5^\circ$ ,  $\Lambda = 200$  nm, and  $f = 0.25$ . Solid lines represent the dispersion relations of the guided modes evaluated including the thin-film dispersion, which is plotted in (b). In contrast, dotted, short-dashed, and long-dashed curves were calculated assuming a constant refractive index equals to 3.434, 3.453, and 3.476, respectively, that correspond to the points with label  $P$  (1020 nm),  $R$  (980 nm), and  $S$  (940 nm) in (b).

cavity [2], intensifying, in comparison with the structure with vertical walls, the interaction between the electromagnetic wave and an active medium that could be inserted in the thin film. The  $Q$ -factor corresponding to the resonance points labeled in Fig. 2, in which the group velocity  $v_g = \omega_1 \equiv d\omega/dk_z$  is zero [2], has been evaluated assuming both a Lorentzian distribution of width  $\delta$  for the initial spatial amplitude  $a_0(z) = 1/(1 + (z/\delta)^2)$  and a quadratic dependence of the frequency  $\omega$  on the wavevector  $k_z$ . Taking into account the definition of the  $Q$ -parameter for a cavity [16], it is straightforward to estimate the quality factor as  $Q = \omega\pi\delta^2/(|\omega_2| \ln 2)$ , where  $\omega_2$  denotes the second derivative of  $\omega$  with respect to  $k_z$  at the point at issue. So, the flatter the dispersion relation, the higher the  $Q$ -factor. We note that the maximum value of  $Q$  is achieved at the point labeled  $a$ . This value can be tuned by changing the air-filling fraction. Accordingly, the  $Q$ -factor is approximately 304 000 for  $f = 0.25$  and  $\theta = 5^\circ$ .

In addition to considering the effect of sloped walls, in a second phase, we have focused attention on the chromatic dispersion of the thin film by inserting the dependence on the frequency of the refractive index in the diagonalization process of our modal method by means of a self-consistency iterative procedure.

Fig. 3(a) shows in detail the effect of the material dispersion on the two upper modes plotted in Fig. 2(b), corresponding to  $\theta = 5^\circ$ , when the thin film is made of  $\text{Al}_{0.12}\text{Ga}_{0.88}\text{As}$ . The material dispersion values have been obtained by fitting experimental data of the refractive index [17], and are shown in Fig. 3(b). Solid lines in Fig. 3(a) denote the modal dispersion relations when the chromatic dispersion of the thin film was considered, while broken lines stand for the results that one can obtain assuming a nondispersive thin-film material with a different value for the refractive index. In the above calculations,  $\Lambda = 200$  nm and  $f = 0.25$ , in such a way that the bandgap is located about 980 nm. At the edge of the Brillouin zone, equivalent to point  $a$  in Fig. 2(b), the  $Q$ -factor changes when the material dispersion is included and now has a value of 346 000. The above results demonstrate that if the material dispersion is neglected, the computed bandgap may exhibit a considerable shift with respect to its actual value.

Conversely, the modification of the slope of the groove walls in photonic crystal waveguides at will permits controlling, within certain limits, the group velocity, or equiv-

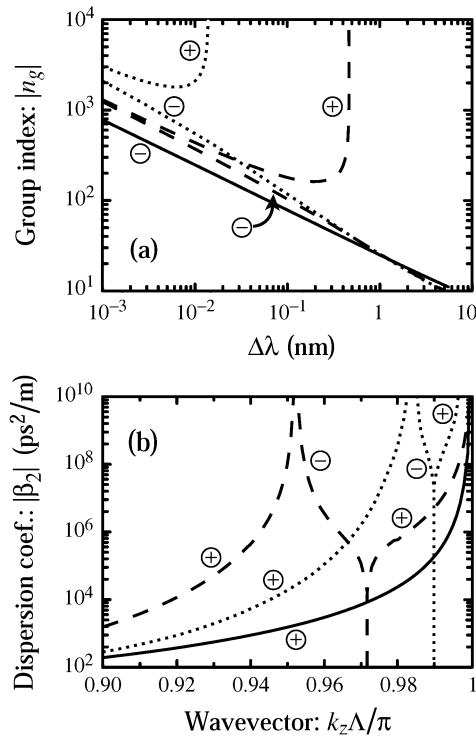


Fig. 4. (a) Group index in terms of the wavelength difference with respect to the band-edge wavelength for the corresponding wall slope, and (b) second-ordered dispersion coefficient versus wavevector. Solid, dotted, and dashed curves correspond to  $\theta = 0^\circ, 5^\circ,$  and  $7.5^\circ,$  respectively. Both the regions of normal ( $\beta_2 > 0$ ) and anomalous ( $\beta_2 < 0$ ) dispersion and the positive and negative sign of the group index are marked with  $\oplus$  and  $\ominus$ , respectively.

alently its inverse, i.e., the group index  $n_g = c/v_g$ ; and the group velocity dispersion,  $D = -2\pi c\beta_2/\lambda^2$ , where  $\beta_2 \equiv d^2k_z/d\omega^2 = -\omega_2/\omega_1^3$  is the second-order dispersion coefficient. The variation of both  $n_g$  and  $\beta_2$  for the upper mode in Fig. 3(a) corresponding to different wall slopes is shown in Fig. 4. Of course, in all cases, the material dispersion is included. Consistently with the divergences that can be observed at the points of zero group velocity (as in [18] and [19]), we have obtained extremely large group velocity dispersions. The high values of dispersion plotted in Fig. 4 strongly depend on the sidewall angle. In fact, tuning the wall slope, the new resonances in both  $n_g$  and  $\beta_2$  change noticeably in position and strength. For instance, in the neighborhood of the Brillouin-zone boundary,  $\beta_2$ , both normal and anomalous, for intermediate values of  $\theta$  is more than two orders of magnitude larger than the values that one can compute for the same structure with vertical walls. According to [20], nonlinear effects could be dramatically strengthened in this case.

In conclusion, we have proved that the slope of the groove walls has a strong influence on the bandgap structure in 1-D photonic crystal waveguides. Therefore, this parameter must be taken into account when studying thin-film photonic crystal devices and it could be exploited as a new design parameter. We have shown that sloped-wall photonic crystal waveguides have quality factors and group velocity dispersions some orders of magnitude larger than those corresponding to the structure with

vertical walls. We have also given evidence that material dispersion should not be ignored. Both the wall tilt and the material dispersion are crucial to analyze and design realistic photonic crystal devices.

## REFERENCES

- [1] T. F. Krauss, R. M. De la Rue, and S. Brand, "Two-dimensional photonic-bandgap structures operating at near infrared wavelengths," *Nature*, vol. 383, pp. 699–702, Oct. 1996.
- [2] D. M. Atkin, P. St. J. Russell, T. A. Birks, and P. J. Roberts, "Photonic band structure of guided Bloch modes in high index films fully etched through with periodic microstructure," *J. Mod. Opt.*, vol. 43, pp. 1035–1053, May 1996.
- [3] O. Painter, R. K. Lee, A. Scherer, A. Yariv, J. D. O'Brien, P. D. Dapkus, and I. Kim, "Two-dimensional photonic band-gap defect mode laser," *Science*, vol. 284, pp. 1819–1821, Jun. 1999.
- [4] C. J. Brooks, G. L. Vossler, and K. A. Winick, "Integrated-optic dispersion compensator that uses chirped gratings," *Opt. Lett.*, vol. 20, pp. 368–370, Feb. 1995.
- [5] W. J. Kim, W. Kuang, and J. D. O'Brien, "Dispersion characteristics of photonic crystal coupled resonator optical waveguides," *Opt. Express*, vol. 11, pp. 3431–3437, Dec. 2003.
- [6] D. W. Prather, "Photonic crystals: An engineering perspective," *Opt. Photonics News*, vol. 13, no. 6, pp. 16–19, Jun. 2002.
- [7] O. J. Painter, A. Husain, A. Scherer, J. D. O'Brien, I. Kim, and P. D. Dapkus, "Room temperature photonic crystal defect lasers at near-infrared wavelengths in InGaAsP," *J. Lightw. Technol.*, vol. 17, pp. 2082–2088, Nov. 1999.
- [8] R. Ferrini, R. Houdré, H. Benisty, M. Qiu, and J. Moosburger, "Radiation losses in planar photonic crystals: Two-dimensional representation of hole depth and shape by an imaginary dielectric constant," *J. Opt. Soc. Amer. B*, vol. 20, pp. 469–478, Mar. 2003.
- [9] W. Bogaerts, P. Bienstman, and R. Baets, "Scattering at sidewall roughness in photonic crystal slabs," *Opt. Lett.*, vol. 28, pp. 689–691, May 2003.
- [10] H.-Y. Ryu, J.-K. Hwang, and Y.-H. Lee, "Effect of size nonuniformities on the band gap of two-dimensional photonic crystals," *Phys. Rev. B*, vol. 59, pp. 5463–5469, Feb. 1999.
- [11] T. N. Langtry, A. A. Asatryan, L. C. Botten, C. M. de Sterke, R. C. McPhedran, and P. A. Robinson, "Effects of disorder in two-dimensional photonic crystal waveguides," *Phys. Rev. E*, vol. 68, no. art. 026611, Aug. 2003.
- [12] T. Asano, M. Mochizuki, S. Noda, M. Okano, and M. Imada, "A channel drop filter using a single defect in a 2-D photonic crystal slab—Defect engineering with respect to polarization mode and ratio of emissions from upper and lower sides," *J. Lightw. Technol.*, vol. 21, no. 5, pp. 1370–1376, May 2003.
- [13] J. A. Monsoriu, M. V. Andrés, E. Silvestre, A. Ferrando, and B. Gimeno, "Analysis of dielectric-loaded cavities using an orthonormal-basis method," *IEEE Trans. Microw. Theory Tech.*, vol. 50, no. 11, pp. 2545–2552, Nov. 2002.
- [14] E. Chow, S. Y. Lin, S. G. Johnson, P. R. Villeneuve, J. D. Joannopoulos, J. R. Wendt, G. A. Vawter, W. Zubrzycki, H. Hou, and A. Alleman, "Three-dimensional control of light in a two-dimensional photonic crystal slab," *Nature*, vol. 407, pp. 983–986, Oct. 2000.
- [15] E. Popov, M. Noeвиère, B. Gralak, and G. Tayeb, "Staircase approximation validity for arbitrary-shaped gratings," *J. Opt. Soc. Amer. A*, vol. 19, pp. 33–42, Jan. 2002.
- [16] A. E. Siegman, *Lasers*: Univ. Science Books, 1986.
- [17] M. A. Fromowitz, "Refractive-index of  $\text{Ga}_{1-x}\text{Al}_x\text{As}$ ," *Solid State Commun.*, vol. 15, pp. 59–63, Jul. 1974.
- [18] V. N. Astratov, R. M. Stevenson, I. S. Culshaw, D. M. Whittaker, M. S. Skolnick, T. F. Krauss, and R. M. De La Rue, "Heavy photon dispersions in photonic crystal waveguides," *Appl. Phys. Lett.*, vol. 77, pp. 178–180, Jul. 2000.
- [19] M. Notomi, K. Yamada, A. Shinya, J. Takahashi, C. Takahashi, and I. Yokohama, "Extremely large group-velocity dispersion of line-defect waveguides in photonic crystal slabs," *Phys. Rev. Lett.*, vol. 87, no. 253902, Dec. 2001.
- [20] B. J. Eggleton, R. E. Slusher, C. M. de Sterke, P. A. Krug, and J. E. Sipe, "Bragg grating solitons," *Phys. Rev. Lett.*, vol. 76, pp. 1627–1630, Mar. 1996.